



## The seasonal change of PAHs in Svalbard surface snow<sup>☆</sup>

Marco Vecchiato<sup>a,b,\*</sup>, Carlo Barbante<sup>a,b</sup>, Elena Barbaro<sup>a,b</sup>, François Burgay<sup>a,c</sup>, Warren RL. Cairns<sup>a,b</sup>, Alice Callegaro<sup>a</sup>, David Cappelletti<sup>b,d</sup>, Federico Dallo<sup>a,b</sup>, Marianna D'Amico<sup>a,b</sup>, Matteo Feltracco<sup>a</sup>, Jean-Charles Gallet<sup>e</sup>, Andrea Gambaro<sup>a,b</sup>, Catherine Larose<sup>f</sup>, Niccolò Maffezzoli<sup>a,b</sup>, Mauro Mazzola<sup>b</sup>, Ivan Sartorato<sup>a,b</sup>, Federico Scoto<sup>a,g</sup>, Clara Turetta<sup>a,b</sup>, Massimiliano Vardè<sup>a,b</sup>, Zhiyong Xie<sup>h</sup>, Andrea Spolaor<sup>a,b</sup>

<sup>a</sup> Department of Environmental Sciences, Informatics and Statistics (DAIS), Ca' Foscari University of Venice, Via Torino 155, 30172, Venezia-Mestre, Venice, Italy

<sup>b</sup> Institute of Polar Sciences - National Research Council (ISP-CNR), Via Torino 155, 30172, Venezia-Mestre, Venice, Italy

<sup>c</sup> Laboratory of Environmental Chemistry (LUC), Paul Scherrer Institut (PSI), 5232, Villigen, Switzerland

<sup>d</sup> Department of Chemistry, Biology and Biotechnology, University of Perugia, 06123, Perugia, Italy

<sup>e</sup> Norwegian Polar Institute, 9296, Tromsø, Norway

<sup>f</sup> Univ Lyon, CNRS, INSA Lyon, Université Claude Bernard Lyon 1, Ecole Centrale de Lyon, Ampère, UMR5005, 69134, Ecully, Cedex, France

<sup>g</sup> Institute of Atmospheric Sciences and Climate - National Research Council (ISAC-CNR), Campus Ecotekne, 73100, Lecce, Italy

<sup>h</sup> Institute of Coastal Environmental Chemistry, Helmholtz-Zentrum Hereon, 21502, Geesthacht, Germany

### ARTICLE INFO

#### Keywords:

PAHs  
Snow  
Arctic  
Winter  
Retene

### ABSTRACT

The Arctic region is threatened by contamination deriving from both long-range pollution and local human activities. Polycyclic Aromatic Hydrocarbons (PAHs) are environmental tracers of emission, transport and deposition processes. A first campaign has been conducted at Ny-Ålesund, Svalbard, from October 2018 to May 2019, monitoring weekly concentrations of PAHs in Arctic surface snow. The trend of the 16 high priority PAH compounds showed that long-range inputs occurred mainly in the winter, with concentrations ranging from 0.8 ng L<sup>-1</sup> to 37 ng L<sup>-1</sup>. In contrast to this, the most abundant analyte retene, showed an opposite seasonal trend with highest values in autumn and late spring (up to 97 ng L<sup>-1</sup>), while in winter this compound remained below 3 ng L<sup>-1</sup>. This is most likely due to local contributions from outcropping coal deposits and stockpiles. Our results show a general agreement with the atmospheric signal, although significant skews can be attributed to post-depositional processes, wind erosion, melting episodes and redistribution.

### 1. Introduction

The Arctic is a remote region marginally affected by the sparse local and indigenous human presence. Nevertheless, significant environmental changes are taking place, due to anthropogenic activities via long-range atmospheric transport (LRAT) of contaminants from North America, Europe, Russia, and Asia (Eneroth et al., 2003; Kosek et al., 2018; Kozak et al., 2013; Law and Stohl, 2007; Oehme et al., 1996). Episodes of Arctic haze accompanied by gaseous air pollution have been observed in winter and spring (Balmer et al., 2019; Stohl et al., 2007), promoted by atmospheric circulation and low temperatures (Abramova et al., 2016). Moreover, there are local sources of pollution in the area

from human settlements (Kallenborn et al., 2017; Vecchiato et al., 2018), abandoned coal mines (Abramova et al., 2018), vehicular traffic (Drotikova et al., 2020), local tourism, and maritime activities (Kozak et al., 2013). Polycyclic aromatic hydrocarbons (PAHs) may derive from the different categories mentioned above, representing useful tracers of the environmental processes involved in the emission, transport and deposition from near and distant sources (Tobiszewski and Namieśnik, 2012).

In this context, as it scavenges PAHs during deposition (Lei and Wania, 2004), snow is an environmental matrix able to capture the contamination signal. One of the major knowledge gaps in investigating PAHs in Arctic snow is seasonality, since most studies are generally

<sup>☆</sup> This paper has been recommended for acceptance by Eddy Y. Zeng.

\* Corresponding author. Department of Environmental Sciences, Informatics and Statistics (DAIS), Ca' Foscari University of Venice, Via Torino 155, 30172 Venezia-Mestre, Venice, Italy.

E-mail address: [vecchiato@unive.it](mailto:vecchiato@unive.it) (M. Vecchiato).

<https://doi.org/10.1016/j.envpol.2023.122864>

Received 27 July 2023; Received in revised form 13 October 2023; Accepted 1 November 2023

Available online 2 November 2023

0269-7491/© 2023 The Authors. Published by Elsevier Ltd. This is an open access article under the CC BY-NC-ND license (<http://creativecommons.org/licenses/by-nc-nd/4.0/>).

conducted in spring (Abramova et al., 2016; Vecchiato et al., 2018), reconstructing conditions during the winter months using snowpits or cores. However, several post-depositional processes, such as revolatilization, degradation and remobilization by winds (Grannas et al., 2013), can alter the original chemical fingerprint, potentially losing the resolution of the obtainable information: as an example, the increasing frequency of winter “rain on snow” (ROS) events, related to climate changes, have a direct impact on the chemical composition of the snowpack, by modifying the distribution of solutes (Spolaor et al., 2021) and PAHs (Kozioł et al., 2017).

The regional sources in the Arctic generally influence the snow composition of PAHs. Total PAH concentrations detected at Summit, Greenland, typically range from  $0.1 \text{ ng L}^{-1}$  to  $10 \text{ ng L}^{-1}$ , accounting for LRAT (Jaffrezo et al., 1994; Masclat et al., 2000). A core retrieved at Site-J, Greenland, showed a marked increase in PAH concentrations over the last 400 years, with low values before the 18th century (mean  $2.3 \text{ ng L}^{-1}$ ) and highest up to  $230 \text{ ng L}^{-1}$  at the end of the 1980 due to anthropogenic emissions (Kawamura and Suzuki, 1994). Higher concentrations ( $\approx 30 \text{ } \mu\text{g L}^{-1}$ ) were found in surface snow from the Ob-Yenisey river watershed, Russia (Melnikov et al., 2003), while in the Novaya Zemlya Archipelago, PAH levels remained below  $30 \text{ ng L}^{-1}$  (Lebedev et al., 2018).

The town of Ny-Ålesund, located in the western part of Spitzbergen in the Svalbard archipelago, is a major research infrastructure for studying Arctic environmental changes and processes (Xie et al., 2015). Previous studies have investigated the presence of PAHs in Svalbard snow (Kozioł et al., 2017) and highlighted the role of long-range transport (Vehviläinen et al., 2002), as well as the influence of local human settlements, such as Ny-Ålesund (Vecchiato et al., 2018), Longyearbyen and Barentsburg (Abramova et al., 2016).

A specific local source of PAHs is represented by coal deposits that have been exploited since the 19th century (Abramova et al., 2016). Unburnt coal particles, both from naturally eroded coal seams and dust emissions from (previous) mining operations, may be found in the soils near the coal deposits (Achten and Hofmann, 2009). The coals of Svalbard were formed from organic material originating predominantly from conifers, and contain high levels of retene (RET; 1-methyl-7-isopropyl phenanthrene) (Ćmiel and Fabiańska, 2004). This compound is also used as a tracer of coniferous wood combustion (Argiriadis et al., 2020). Previous determinations of RET in Arctic snow and atmospheric samples generally considered this compound as a pure softwood combustion tracer (Macdonald et al., 2000; Masclat et al., 2000). In Ny-Ålesund the occurrence of coal-derived PAHs was previously detected in snow, with levels of RET up to  $1.8 \text{ } \mu\text{g L}^{-1}$ , while the sum of the other PAHs ranged from  $2.6$  to  $299 \text{ ng L}^{-1}$  (Vecchiato et al., 2018). In the same area the influence of coal was also detected in soil (Na et al., 2021), lake and marine sediments (Kim et al., 2011; Pouch et al., 2017). Concentrations of the sum of PAHs (not including RET) were found ranging at  $803$ – $6244 \text{ ng g}^{-1}$  (at 5% TOC) in terrestrial sediments collected close to the coal mine of Ny-Ålesund, but with lower levels at increasing distances from the mine (Steenhuisen and van den Heuvel-Greve, 2021).

The present study represents the first yearly monitoring campaign of PAHs in Arctic surface snow carried out in Ny-Ålesund, Svalbard Archipelago, from early autumn 2018 to the spring melt period in 2019 at a weekly temporal resolution, therefore including winter months. While comparable seasonal information is available for aerosol samples collected at the nearby Zeppelin observatory (ebas.nilu.no), giving a detailed description of the yearly behavior of PAHs in the atmosphere, contemporary records of their distribution in the snow are not available. In this work we aim to better elucidate the sources and processes that control PAH concentrations in snow, in terms of both long-range and local scales. Therefore, this work aims to identify:

- how the atmospheric PAH signal is actually recorded in the snow deposition;

- how post-depositional processes and local conditions may affect this record.

The final goal is to fill a knowledge gap between information from atmospheric studies and the data retrievable from snow-pits and cores to support the reconstruction of environmental and paleoclimatic trends of organic compounds archived in the cryosphere.

## 2. Materials and methods

### 2.1. Characteristics of the sampling site

Surface snow samples were collected close to the Gruvebadet Aerosol Laboratory ( $78.91622^{\circ}\text{N}$   $11.89536^{\circ}\text{E}$ , Ny-Ålesund, Svalbard Archipelago) into stainless-steel containers pre-cleaned with pesticide-grade acetone and *n*-hexane. Four snow poles were fixed to the ground at the beginning of the season to delimit the sampling snow field, where to regularly measure the snow height and its accumulation rate. Sampling was performed down to a depth of 20 cm from the snow surface, during the period going from 4<sup>th</sup> October 2018 to 13<sup>th</sup> May 2019. Overall 35 samples were collected, with an approximately weekly resolution. The sampling site was located in a restricted areas not directly affected by local emissions from the activities in the town of Ny-Ålesund (Feltracco et al., 2021).

### 2.2. Sample preparation and analysis

Samples were collected into stainless-steel containers pre-cleaned with pesticide-grade acetone and *n*-hexane and were allowed to melt at room temperature in the laboratories of the CNR Arctic Station Dirigibile Italia, obtaining 500 mL–660 mL (580 mL on average) of water, and extracted using 200 mg Oasis® HLB cartridges (Waters Corp., Milford, MA USA) following previously developed methods (Vecchiato et al., 2020, 2018). Samples were spiked with phenanthrene  $^{13}\text{C}$  (Cambridge Isotope Laboratories, Andover, MA USA) as an internal standard. The cartridges were then stored at  $-20^{\circ}\text{C}$  and were later eluted using 1 mL of toluene, 15 mL of dichloromethane and 10 mL of *n*-hexane (pesticide-grade, Romil Ltd). This operation took place in the stainless steel organic free clean-room (class 10,000) at the Ca' Foscari University of Venice (Italy).

Instrumental analyses for native PAHs (naphthalene (NAP), acenaphthylene (ACY), acenaphthene (ACE), fluorene (FLU), phenanthrene (PHE), anthracene (ANT), fluoranthene (FLA), pyrene (PYR), benzo(a)anthracene (BaA), chrysene (CHR), retene (RET), benzo(b)fluoranthene (BbF), benzo(k)fluoranthene (BkF), benzo(e)pyrene (BeP), benzo(a)pyrene (BaP), perylene (PER), dibenzo(a,h)anthracene (DahA), indeno(1,2,3-c,d)pyrene (IcdP) and benzo(ghi)perylene (BghiP); Dr. Ehrenstorfer (Augsburg, Germany)) were conducted by GC-MS/MS (Trace 1310 - TSQ 9000 Thermo Fisher) using a 60-m HP-5MS column (0.25 mm I.D., 0.25  $\mu\text{m}$ ; Agilent Technologies). Instrumental conditions used to identify and quantify each PAH are reported in table S11. The performances of the analytical method were evaluated preparing synthetic samples spiking 50 L of a dichloromethane solution containing the native PAHs at  $1 \text{ ng L}^{-1}$  each into 0.5 L of ultrapure water for organic analyses (Purelab Flex; ELGA LabWater) and then following the procedure described above. Internal standard ( $50 \text{ } \mu\text{l}$  of  $^{13}\text{C}$  PHE at  $1 \text{ ng L}^{-1}$ ) was added respectively at the beginning of the procedure to perform trueness tests ( $n^{\circ} = 3$ ; Table S11) or after the final concentration to calculate the recovery rates ( $n^{\circ} = 3$ ; Table S11). Results were mean-blank corrected, and the method detection limits (MDLs) were calculated as three times the standard deviation of the blank signals (Table S11).

To study the source region of the air masses reaching the Gruvebadet Aerosol Laboratory, back-trajectories were computed using the NOAA-HYSPLIT model 5.0.0 (Stein et al., 2015). The trajectories were calculated for 120 h, starting every 6 h at 10 m above ground level (AGL) with backward direction using vertical velocity and NCEP/NCAR reanalysis

database (horizontal resolution of 278 km), according to previous studies on atmospheric circulation in the same site (Feltracco et al., 2021). The frequency analyses were conducted for the periods spanning between each sampling interval (approximately one week), covering the whole season (see Fig. 1).

### 3. Results and discussion

The analyzed PAH compounds show marked seasonal trends during the study period (Fig. 2). RET was the analyte with the highest concentrations, of up to  $97 \text{ ng L}^{-1}$ , but it significantly decreased during the winter and remained minimum until spring. The other PAHs generally showed an opposite trend with the highest levels in winter, however presenting minor relative peaks in autumn and spring concurrent to RET (Fig. 2). The sum of the 16 high priority PAHs resulted overall lower than RET during the sampling period, with values ranging between  $0.76 \text{ ng L}^{-1}$  and  $37 \text{ ng L}^{-1}$  (Table SI2).

#### 3.1. Trends and sources of retene

RET peaked at the beginning of the sampling season ( $97 \text{ ng L}^{-1}$  on 19<sup>th</sup> October 2018) and it started to decrease from the end of October to mid-December (Fig. 2). During the whole winter and the beginning of spring, RET values remained below  $3 \text{ ng L}^{-1}$ . Concentrations increased again in May, reaching a value of  $82 \text{ ng L}^{-1}$ . The behaviour observed for this tracer may be explained by considering its possible sources: RET is the dominant PAH component in Svalbard coals: its presence is linked to the geology of the islands and the coal outcrops observed in several geological formations near Ny-Ålesund (Ćmiel and Fabiańska, 2004). The resulting interpretation is that when the snow coverage of the area is absent or patchy, coal and soil particles may be transported to nearby snowfields, bringing RET and, more local PAH contamination. Conversely, in winter, as long as the surrounding area remains covered by snow and ice, this process is prevented, and the LRAT inputs of PAHs become predominant in the air and snow. Therefore, high values of RET found in the snow samples suggest that soil and dust deposition from local coal stockpiles near Ny-Ålesund may be the principal contributors of PAHs deposited in the area at the beginning (until the 17<sup>th</sup> December 2018) of and the end of the sampling season (after 1<sup>st</sup> May 2019) (Fig. 2). In the snow-covered period, the role of local sources becomes less important, and the other PAHs detected in the samples may be mainly attributed to long-distance sources.

RET was previously detected in marine sediments in the Kongsfjord–Krossfjord system facing Ny-Ålesund, where it was used as an indicator for coal-derived organic matter (Kim et al., 2011). In the surface snow around the town of Ny-Ålesund, RET had a broader range of concentrations ( $2.6 \text{ ng L}^{-1}$  -  $1.8 \mu\text{g L}^{-1}$ ) compared to the Gruvebadet samples, while still showing a clear prevalence over  $\sum_{16}$  PAHs and accounting for local inputs (Vecchiato et al., 2018). It should be underlined

that, along with the other PAHs, RET may still derive from long-range sources, such as combustion of coniferous wood in lower latitudes, however, as discussed more in detail in paragraph 3.4, the concentrations of atmospheric RET at the Zeppelin observatory result at orders of magnitude lower than the other major PAHs, and with a typical peak of concentrations occurring in late January (ebas.nilu.no). Therefore, the deposition of atmospheric RET cannot explain its higher concentrations in comparison to the other PAHs detected for this compound in the snow at Gruvebadet, nor its seasonal trends. Moreover, no significant soft-wood fires were reported in the Ny-Ålesund area during the sampling campaign and even unknown local contamination from the town is prevented to affect the snow sampling area, since main winds flow parallel to the fiord towards the ocean (Feltracco et al., 2021; Ferrero et al., 2016; Vecchiato et al., 2018). Consequently, coal represents the only established source of RET characterizing the whole area through deposits, soil, dust, and natural outcrops, apart from the winter months, when the extended snow cover prevents the resuspension of these materials.

Results show that the distribution of RET can be considered as a tracer of the local sources and as a secondary tracer of surface snow coverage. However, this should be considered only valid in those regions where outcropping coals are strongly characterized by RET and only if the comparison with the other PAHs reflects a dominating fingerprint typical of this peculiar source. RET in snow samples collected in areas unaffected by these coal sources should still be considered a marker of coniferous wood combustion (Masclat et al., 2000).

#### 3.2. Temporal variability of priority PAHs

At the beginning of the season, from October to early December, the  $\sum_{16}$  PAHs concentrations were relatively low, at a few  $\text{ng L}^{-1}$  (Table SI2). As reported by the trend of the snowpack height and of the surface snow temperature (Fig. 2), snow deposition was affected by melting episodes, due to the occurrence of repeated ROS events and temperatures above  $0 \text{ }^\circ\text{C}$ . High temperatures largely affected the snowpack with melting, ablation and redistribution of the snow, also disturbing the composition of the PAH signal leading to relatively higher concentrations on October 19<sup>th</sup> and November 23<sup>rd</sup>. The samples collected in this period were probably reflecting amplification phenomena (Meyer and Wania, 2008) and/or internal redistribution of PAHs in the snowpack: indeed there was a higher contribution of NAP, which is a light and more water-soluble compound that was previously found to be enriched in wet snow layers (Kozioł et al., 2017), representing the 44–63 % of the  $\sum_{16}$  PAHs amount when detected in the samples between October 19<sup>th</sup> and December 4<sup>th</sup>. In the following samples of December NAP represented only the 5–28 % of the amount of  $\sum_{16}$  PAHs.

Concentrations of heavy PAHs started to increase from 12<sup>th</sup> to 17<sup>th</sup> December, when  $\sum_{16}$  PAHs have concentrations of  $12 \text{ ng L}^{-1}$  and  $9.7 \text{ ng}$



Fig. 1. Location of the surface snow samplings, with indication of the relevant sites in the area. Photo: courtesy of A. Spolaor.

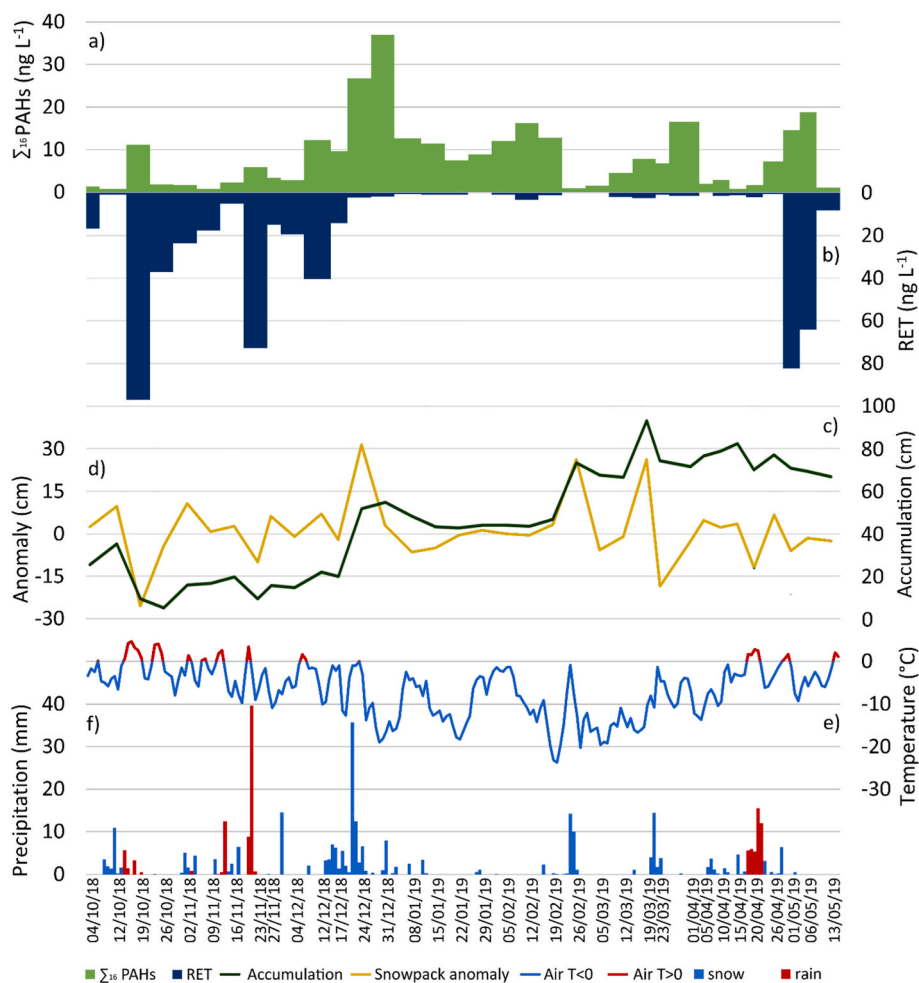


**Fig. 2.** Concentrations of  $\Sigma_{16}$  PAHs (green bars; 1a) and RET (blue bars; 1b) (ng L<sup>-1</sup>) detected in the snow samples. The accumulation (snow height, cm; green curve; 1c) and the weekly variation (Anomaly:  $H_{\text{snow}}t^0 - H_{\text{snow}}t^{-1}$ , cm; yellow curve; 1d) of the snowpack profile were calculated as the average of five measurements at the time of each sampling. Average daily air temperature (°C) and precipitation of snow/rain (blue/red; mm) for Ny-Ålesund were retrieved from [www.yr.no](http://www.yr.no). (For interpretation of the references to colour in this figure legend, the reader is referred to the Web version of this article.)

L<sup>-1</sup>, respectively. These values still corresponded to relevant levels of RET, somehow representing a connecting period between the autumnal and the winter snow conditions, potentially reflecting the influence of both local and long-range sources in the samples. More relevant were the depositions at the end of December: the increase of  $\Sigma_{16}$  PAHs on December 24th coincided with an increase in snowpack thickness of about 30 cm following fresh heavy snowfalls (Fig. 2). Concentrations peaked at 37 ng L<sup>-1</sup> on December 31st. Meanwhile, the levels of RET dropped, discounting the possible hypothesis of relevant PAH contributions from the local sources. This major peak of PAHs registered in the precipitation event was therefore significantly linked to long-range sources of contamination.

In the following period (January 8th – February 19th), the  $\Sigma_{16}$  PAHs concentrations ranged between 7 ng L<sup>-1</sup> and 16 ng L<sup>-1</sup>, showing lower values on January 22nd and 29th, when PHE resulted below the MDL (Table SI2). During this period, the formation of wind crusts was observed on the snow surface at the Gruvebadet station. The height of the snowpack remained constant during this month (Fig. 2c and d). Most of the samples collected between January and February were therefore mostly referring to the same previous snow precipitation. However, it is possible to notice a relative increase in PAH concentrations from January 22nd to February 12th. Considering the almost total absence of snow precipitation in this period (Fig. 2), this increase, less pronounced than the event at the end of December, suggests a possible contribution from the dry deposition of atmospheric PAHs, constituting a less

efficient process than wet scavenging. This hypothesis would be also consistent with the high atmospheric PAH levels detected at Zeppelin in that period (section 3.4). The sample collected on February 26th was instead referring to the second main snow deposition event (Fig. 2), but, contrary to the previous one,  $\Sigma_{16}$  PAHs concentrations dramatically dropped to 0.86 ng L<sup>-1</sup>. Since in this case the snow deposition was significantly less polluted, the air masses encountered during snow formation and deposition should have been less influenced by the PAH emitting sources in lower latitudes. A remarkable difference distinguishes the two main snow deposition events that occurred during the sampling campaign, taking place respectively at the end of December and at the end of February. Both events brought an increase in the snow height of approximately 30 cm. Notably, while a significant increase in the concentrations corresponded to the first episode (Fig. 2), remaining relatively high ( $\Sigma_{16}$  PAHs: 7.5–37 ng L<sup>-1</sup>) until February 19th, after the second event, PAHs fell by one order of magnitude ( $\Sigma_{16}$  PAHs: 0.86 ng L<sup>-1</sup>). This substantial difference is likely reflecting a variation in the origin of the air masses reaching Svalbard in the period before sampling. According to the HYSPLIT frequency analysis of the back-trajectories, the polluted sample collected on Dec 24th was influenced by sources placed in northern Europe (Fig. SI1a). Atmospheric PAH sources to the Norwegian Arctic are known to originate in the circumpolar countries, with the higher concentrations in winter and spring mainly deriving from western Russia and northern Europe (Balmer et al., 2019). Conversely, the air masses preceding Feb 26th came mainly from the

Arctic Ocean and Greenland (Fig. S11c) transporting clean air and contributing to the deposition of relatively clean snow.

The samples collected in March and April showed a more complex behaviour, due to repeated snow depositions, wind-driven erosion and redistribution, together with rain events, and temperatures above 0 °C, which became more frequent from late April onwards (Fig. 2). Remarkably, NAP showed its highest peak on April 1st (10 ng L<sup>-1</sup>), no peculiar meteorological conditions characterizing the sample. We may suppose the occurrence of amplification phenomena due to the possible internal redistribution and accumulation of this hydrophilic compound

inside the snowpack (Kozioł et al., 2017), or the actual deposition of NAP-enriched snow.

In May, melting accelerated: despite the height of the snowpack in the sampling area remaining thoroughly stable (Fig. 2), ice lenses resulted visible in the profile. Moreover, the snow coverage of the surroundings, including the road, coal deposits and outcroppings (Fig. S12), started to become patchy, exposing soil and dust that were spread over the area, leading to the spring peak of RET observed in the samples. Consequently, considering that coal is a source of both RET and the other PAHs (Ćmiel and Fabiańska, 2004; Steenhuisen and van den

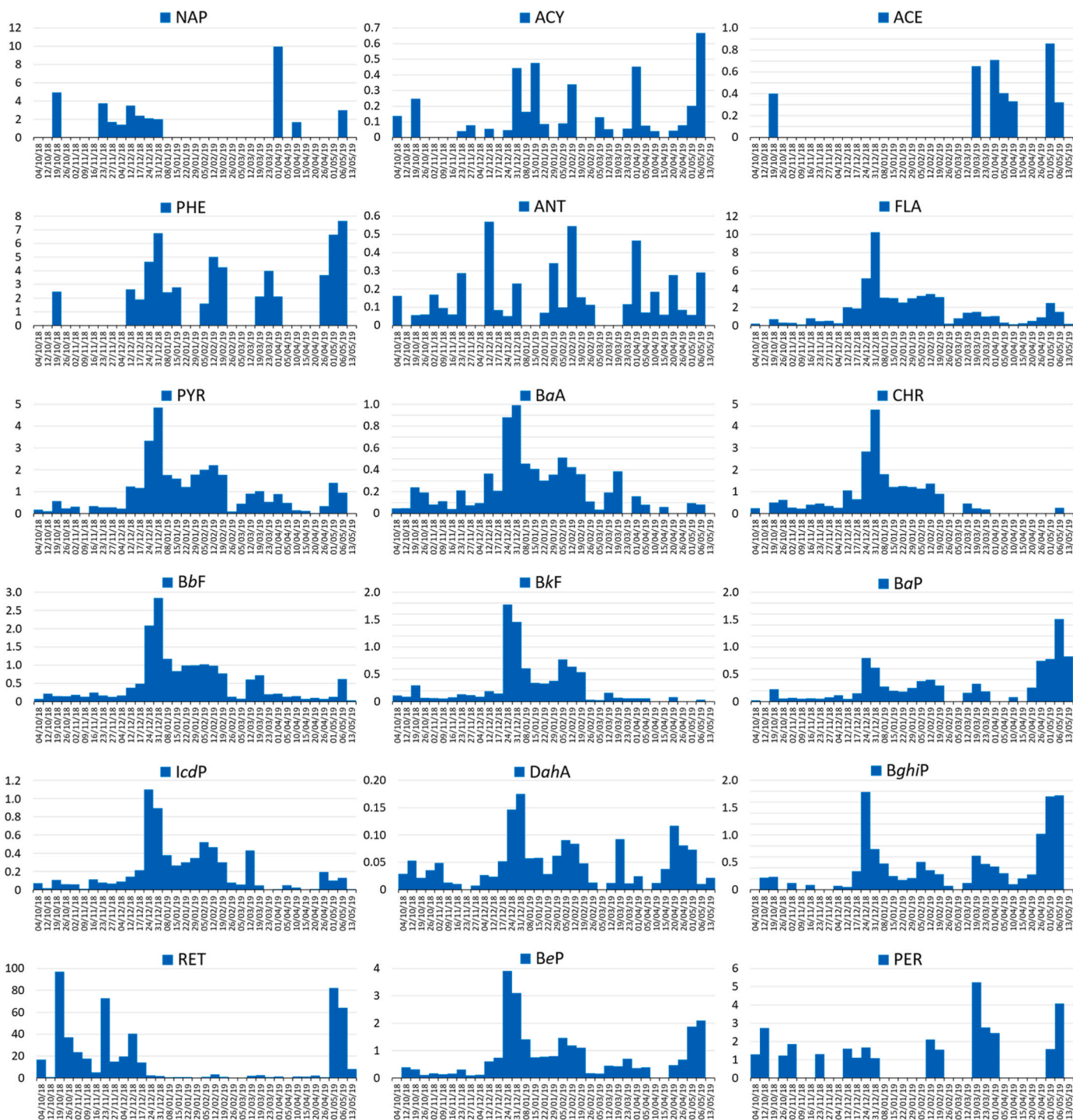


Fig. 3. concentration profiles of the analyzed PAHs reported in ng L<sup>-1</sup>. Note different scales. FLU resulted below detection limits in every sample and is not displayed.

Heuvel-Greve, 2021), local sources may also be considered relevant for the May snow depositions, when levels of  $\sum_{16}$  PAHs of up to  $19 \text{ ng L}^{-1}$  were detected.

The concentration levels of PAHs in snow at the Gruvebadet site ( $\sum_{16}$  PAHs:  $0.76\text{--}37 \text{ ng L}^{-1}$ ) result lower than those previously found for contaminated “urban” samples inside the Ny-Ålesund settlement ( $\sum_{16}$  PAHs up to  $299 \text{ ng L}^{-1}$ ), while being comparable to the background snow samples not influenced by the town ( $\sum_{16}$  PAHs:  $2.6\text{--}23 \text{ ng L}^{-1}$ ) (Vecchiato et al., 2018). These values are similar to those reported at Summit, Greenland, with total PAHs resulting at  $0.6\text{--}2.4 \text{ ng L}^{-1}$  (Jaffrezo et al., 1994) and fall in the lower range of those found on the Foxfonna glacier, Svalbard, where concentrations up to  $4 \mu\text{g L}^{-1}$  were detected (Kozioł et al., 2017). High values were found in contaminated snow from the area of Longyearbyen and Barentsburg, with the sum of PAHs resulting at  $2\text{--}119 \mu\text{g g}^{-1}$  in the particulate material filtered from the snow (Abramova et al., 2016).

The highest values of PAHs found in the snowpack are associated with specific transport and precipitation events linked to low-pressure systems, which are able to promote the transfer of pollutant-laden air masses from the mid-latitudes towards the Svalbard area. Such transport events are also generally characterized by intense snowfall and/or liquid precipitation, causing ROS events, and are expected to increase in the future, due to the slowing of the polar vortex due to climate change (Spolaor et al., 2021).

### 3.3. The composition of the PAH pattern

The detailed trends of the individual PAH compounds are reported in Fig. 3. Focussing on the individual PAHs analyzed in the surface snow at Gruvebadet, the concentration profiles are dominated by FLT and PHE (Table SI2), accounting on average for 20% and 13% of the  $\sum_{16}$  PAHs respectively, followed by PYR (12%) and NAP (12%). The remaining PAHs detected are on average below 10%. The sum of FLT, PHE, PYR, and NAP constitutes more than 50% of the  $\sum_{16}$  PAHs analyzed, and FLT, PHE, and PYR were detected in more than 50% of the samples. The different PAHs show dissimilar seasonal behaviour (Fig. 3). Some light compounds, such as NAP, which was found in relatively high concentrations in some samples, were detected occasionally and/or without a defined seasonal evolution. Many heavier PAHs (e.g., FLT, CHR or IcdP) are instead characterized by a bell-shaped profile, peaking at the end of December (Fig. 3), while other compounds (e.g., BaP and BghiP) present a second peak in May.

In addition to the 16 priority PAHs, and beyond RET that has already been discussed, also PER and BeP were detected in the samples, with concentrations up to  $5.2 \text{ ng L}^{-1}$  and  $3.9 \text{ ng L}^{-1}$ , respectively. If PER seems independent from any specific trend, suggesting quite constant diagenetic sources for this compound, BeP instead followed a seasonal pattern similar to its isomer BaP (Fig. 3).

Diagnostic ratios of PAHs are powerful tools used for the determination of the emission sources in urban areas (Sun et al., 2022; Zhang et al., 2021, 2020), however, their reliability has been questioned when applied to remote regions (Katsoyiannis and Breivik, 2014). Contradictions between diagnostic ratios may be related to the different reactivities of the isomers during atmospheric transport, suggesting opposing PAH sources in snow depositions (Vecchiato et al., 2020). However, the BaP/(BaP + BeP) ratio is specifically based on the more rapid atmospheric degradation of BaP compared to BeP, therefore providing an indication on the age of the air masses and discriminating local sources (fresh particles  $\sim 0.5$ ) from long-range sources (aged particles  $<0.5$ ) (Tobiszewski and Namieśnik, 2012). In our samples the BaP/(BaP + BeP) ratio shows a pronounced seasonal variation (Fig. SI3), resulting close to 0.5 in autumn and spring, but with lower values in winter, indicating the predominance of aged particles. This consequently confirms that long-range transport and snow deposition of PAHs occurs mainly during winter.

In different studies conducted in the Svalbard Archipelago, NAP

frequently resulted the major PAH amongst those analyzed in snow (Vehviläinen et al., 2002) and freshwater (Kosek et al., 2018; Kozak et al., 2017; Lehmann-Konera et al., 2020; Polkowska et al., 2011). In our samples, NAP resulted the most abundant component among the 16 priority PAHs in 8 out of the 11 samples where it resulted above the MDL (Table SI2). We should underline that the blanks of this analyte are about 1-2 orders of magnitude higher than the other PAHs (Table SI1), therefore potentially underrepresenting its actual distribution. Nevertheless, NAP resulted lower than PHE and FLA in the late December event (Table SI2). The same preponderance of 4-ring PAHs over NAP was characteristic of snow at Summit, Greenland (Jaffrezo et al., 1994). In the freshwater from southern Svalbard the predominance of NAP over heavier PAHs was highly variable on limited temporal (Kosek et al., 2018; Kozak et al., 2017) and spatial (Lehmann-Konera et al., 2020; Polkowska et al., 2011) scales.

### 3.4. Comparison between snow and atmospheric PAHs

The monitoring of PAHs in aerosol at the nearby Zeppelin observatory, which are not part of our analyses but are freely available at ebas.nilu.no, gives us the opportunity to compare the trends registered in the surface snow, with those characterising the atmospheric composition during the same period. It should be noted that the Zeppelin station is located about 400 m above the Gruvebadet Aerosol Laboratory, lying above the atmospheric boundary layer for most of the time, therefore it is generally unaffected by local sources (Balmer et al., 2019; Stohl et al., 2007; Yu et al., 2019). The  $\sum_{16}$  PAHs in the atmosphere resulted in concentrations up to  $3.2 \text{ ng m}^{-3}$ , showing a defined bell-shaped pattern (Fig. 4), peaking in winter and being largely dominated by Low Molecular Weight (LMW; 2–3 rings) PAHs: NAP and FLU on average account for 63% and 26% of the atmospheric  $\sum_{16}$  PAHs, respectively. The snow profile is instead generally shifted towards the High Molecular Weight (HMW;  $\geq 4$  rings) PAHs (Fig. 4), mostly PHE, FLT and PYR. This difference between atmospheric and snow composition could be explained considering the different physical-chemical properties of PAHs leading to differential phase distribution (Lei and Wania, 2004): with the lowering of the temperatures, while NAP tends to remain in the gaseous phase, the other heavier PAHs tend to adsorb to particles and to snow surfaces. Consequently, for temperatures below  $0 \text{ }^\circ\text{C}$ , while the dominant atmospheric deposition process for NAP is largely represented by dry gaseous deposition, higher proportions of the other compounds tends to be wet-deposited after being adsorbed to snowflakes or through particle scavenging (Grannas et al., 2013; Lei and Wania, 2004). Consistently, we obtained the shift of the patterns shown in Fig. 4. However, the dominant mechanism of atmospheric deposition is strongly dependent on phase composition, kinetic parameters and temperature, therefore it results highly variable after limited environmental changes (Lei and Wania, 2004).

During summer melting, while the more hydrophilic NAP tends to be transported with the snowmelt, there is a higher repartition of the heavier PAHs to the less mobile organic matter and soil particles (Casal et al., 2018; Meyer and Wania, 2008). Consequently, a relative NAP dominance of the pattern is frequently detected in freshwater (Kozak et al., 2017; Lehmann-Konera et al., 2020; Li et al., 2020).

Comparing the different seasonal profiles of PAHs, the main event registered in snow at the end of December (Figs. 2 and 4) finds correspondence with a simultaneous spike of PAH concentrations in the atmosphere. However, the highest levels of PAHs in aerosol samples were registered between the end of January and early February. This is consistent with the literature (Balmer et al., 2019) and with the corresponding back-trajectory frequencies, which result as significantly deriving from northern Europe (Fig. SI2b) during that period. Despite this, the trend in snow remained at relatively lower concentrations during the same weeks, due to the action of winds, removing fresh snow deposition and leading to the above-mentioned formation of surface wind crust. This means that even the major events of LRAT of

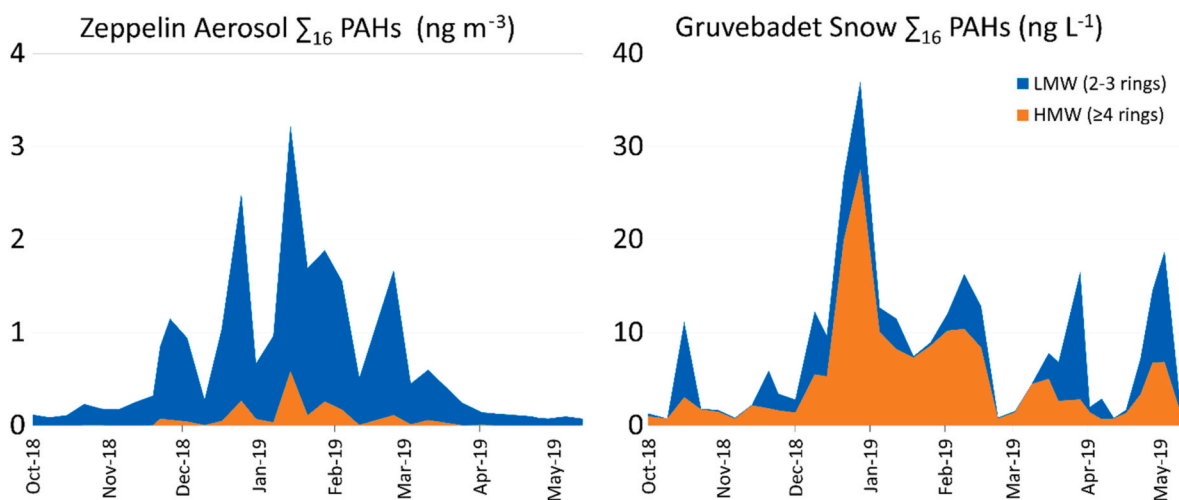


Fig. 4. Seasonal distribution of the  $\Sigma_{16}$  PAHs among the Low Molecular Weight (LMW; 2–3 rings) and High Molecular Weight (HMW;  $\geq 4$  rings) compounds observed in the atmosphere ( $\text{ng m}^{-3}$ ) at the Zeppelin station (ebas.nilu.no) and in the snow ( $\text{ng L}^{-1}$ ) at the Gruvebadet observatory.

contaminants may remain almost unrecorded in deposition, resulting in decoupled signals from the two matrices, air and snow. Consequently, potential profiles taking place in late-season snow-pits may misrepresent the actual contamination trends, if the post-depositional phenomena occurring on the ground are not considered.

Notably RET was also present in the aerosol Zeppelin samples, being detected between the end of November and the beginning of February, at levels (median  $0.0019 \text{ ng m}^{-3}$ ) two orders of magnitude lower than NAP (median  $0.18 \text{ ng m}^{-3}$ ) (ebas.nilu.no). These concentrations of RET were representing only the 0.1–0.5 % of the corresponding  $\Sigma_{16}$  PAHs in the aerosol samples. In comparison to the other PAHs, the low atmospheric concentrations of RET and its seasonal distribution indicate that at Zeppelin it derives most likely from long-range softwood burning, rather than from the local coal sources, whose fingerprint is instead characterized by a dominance of RET above the  $\Sigma_{16}$  PAHs.

Similarly, the bell-shaped profiles detected in the snow for most of the heavy PAHs, including FLA, PYR, BaA, CHR, BbF, BkF and IcdP (Fig. 3) correspond to the atmospheric trends, reflecting long-range inputs occurring mainly in the central winter months. Other heavy compounds, namely BaP, BeP and BghiP, in addition to this winter peak, show a late spring increase, which is otherwise likely due to local contamination, coinciding with the RET peak and with the above mentioned relatively high BaP/(BaP + BeP) ratios. This confirms that the major sources of PAHs on the snowpack may attributed to local or long-range inputs considering different sampling seasons.

#### 4. Conclusions

One of the main features characterizing the yearly trend of PAHs in Arctic surface snow is the significant variability of their seasonal profiles. While RET may reach relatively high concentrations in autumn and spring due to its natural occurrence in local coals, during winter the contributions from LRAT sources become dominant for the other PAHs, in parallel with their atmospheric trends. Snow depositions preserve the fundamental patterns of the  $\Sigma_{16}$  PAH trends, reporting higher levels in winter. However, referring to the initial objectives of this study, some key aspects should be considered, since weather conditions may lead to a divergence of the signal recorded in the snowpack.: I) Winds can potentially remove or redistribute fresh snow, while rain events can cause melting and differential vertical movements of PAHs. II) The actual deposition of PAHs in the snow depends on the combination of the origin of the air masses, e.g., from uninhabited areas or from contaminated lower latitudes, with the actual occurrence of events of snow precipitation, scavenging the contaminants from the air more

efficiently than dry depositions. III) Another key element is represented by the shift of the PAH pattern towards heavier compounds during aerosol scavenging, bringing uneven signals between atmosphere and snow. Moreover, in the areas where seasonal melting occurs, this is also likely followed by a consecutive shift of the pattern, leading to a prevalence of the most hydrophilic PAHs in the freshwaters. These fundamental issues should be considered for the interpretation of the record of a tracer from a late-winter or spring snow-pit, as well as for the analyses of organics in ice cores, especially when collected in glaciers with high summer ablation.

In this context, the severe climatic changes currently observed in the Arctic will affect the framework of the distribution of PAHs in snow. This can occur both through influencing adsorption and scavenging equilibria, which are highly temperature-dependent, but also bringing more frequent warm rains damping the chemical signals recorded in snow deposition.

#### CRediT authorship contribution statement

**Marco Vecchiato:** Methodology, Formal analysis, Investigation, Data curation, Visualization, Writing – original draft. **Carlo Barbante:** Supervision, Project administration, Funding acquisition. **Elena Barbato:** Formal analysis, Investigation, Data curation. **François Burgay:** Formal analysis, Investigation, Data curation. **Warren RL Cairns:** Investigation, Data curation. **Alice Callegaro:** Conceptualization, Investigation. **David Cappelletti:** Investigation. **Federico Dallo:** Investigation. **Marianna D’Amico:** Formal analysis, Data curation. **Matteo Feltracco:** Investigation, Data curation. **Jean-Charles Gallet:** Investigation. **Andrea Gambaro:** Methodology, Investigation, Resources. **Catherine Larose:** Investigation, Data curation. **Nicolò Maffezzoli:** Investigation, Data curation. **Mauro Mazzola:** Investigation. **Ivan Sartorato:** Investigation. **Federico Scoto:** Formal analysis, Investigation. **Clara Turetta:** Resources. **Massimiliano Vardè:** Investigation. **Zhiyong Xie:** Investigation. **Andrea Spolaor:** Conceptualization, Project administration, Funding acquisition, Writing – review & editing.

#### Declaration of competing interest

The authors declare that they have no known competing financial interests or personal relationships that could have appeared to influence the work reported in this paper.

## Data availability

Data will be made available on request.

## Acknowledgements

This project has received funding from the European Union's Horizon 2020 research and innovation programme under grant agreement no. 689443 via ERA-PLANET Strand 4 project iCUPE (Integrative and Comprehensive Understanding on Polar Environments). We are grateful to the Arctic Station Dirigibile Italia from the Italian National Research Council – Institute of Polar Science (CNR-ISP) for logistical support. We acknowledge the help of ELGA LabWater in providing the PURELAB Pulse and PURELAB Flex, which produced the ultrapure water used in these experiments.

## Appendix A. Supplementary data

Supplementary data to this article can be found online at <https://doi.org/10.1016/j.envpol.2023.122864>.

## References

- Abramova, A., Chernianskii, S., Marchenko, N., Terskaya, E., 2016. Distribution of polycyclic aromatic hydrocarbons in snow particulates around Longyearbyen and Barentsburg settlements, Spitsbergen. *Polar Rec.* 52, 645–659. <https://doi.org/10.1017/S0032247416000243>.
- Abramova, A., Semenov, I., Chernyanskiy, S., Ogorodov, S., 2018. Concentration of trace elements in soils historically affected by coal mining in svalbard. In: *International Multidisciplinary Scientific GeoConference Surveying Geology and Mining Ecology Management. SGEM*, pp. 251–258. <https://doi.org/10.5593/sgem2018/5.2/S20.033>.
- Achten, C., Hofmann, T., 2009. Native polycyclic aromatic hydrocarbons (PAH) in coals – a hardly recognized source of environmental contamination. *Sci. Total Environ.* 407, 2461–2473. <https://doi.org/10.1016/j.scitotenv.2008.12.008>.
- Argiriadis, E., Martino, M., Segnana, M., Poto, L., Vecchiato, M., Battistel, D., Gambaro, A., Barbante, C., 2020. Multi-proxy biomarker determination in peat: optimized extraction and cleanup method for paleoenvironmental application. *Microchem. J.* 156, 104821 <https://doi.org/10.1016/j.microc.2020.104821>.
- Balmer, J.E., Hung, H., Yu, Y., Letcher, R.J., Muir, D.C.G., 2019. Sources and environmental fate of pyrogenic polycyclic aromatic hydrocarbons (PAHs) in the Arctic. *Emerging Contam.* 5, 128–142. <https://doi.org/10.1016/j.emcon.2019.04.002>.
- Casal, P., Cabrerizo, A., Vila-Costa, M., Pizarro, M., Jiménez, B., Dachs, J., 2018. Pivotal role of snow deposition and melting driving fluxes of polycyclic aromatic hydrocarbons at coastal Livingston island (Antarctica). *Environ. Sci. Technol.* 52, 12327–12337. <https://doi.org/10.1021/acs.est.8b03640>.
- Ćmiel, S.R., Fabiańska, M.J., 2004. Geochemical and petrographic properties of some Spitsbergen coals and dispersed organic matter. *Int. J. Coal Geol.* 57, 77–97. <https://doi.org/10.1016/j.coal.2003.09.002>.
- Drotikova, T., Ali, A.M., Halse, A.K., Reinardy, H.C., Kallenborn, R., 2020. Polycyclic aromatic hydrocarbons (PAHs) and oxy- and nitro-PAHs in ambient air of the Arctic town Longyearbyen , Svalbard. *Atmos. Chem. Phys.* 20, 9997–10014.
- Eneroth, K., Holm, K., Kjellström, E., 2003. A trajectory climatology for Svalbard; investigating how atmospheric flow patterns influence observed tracer concentrations. *Phys. Chem. Earth* 28, 1191–1203. <https://doi.org/10.1016/j.pce.2003.08.051>.
- Feltracco, M., Barbaro, E., Spolaor, A., Vecchiato, M., Callegaro, A., Burgay, F., Vardé, M., Maffezzoli, N., Dallo, F., Scotto, F., Zangrando, R., Barbante, C., Gambaro, A., 2021. Year-round measurements of size-segregated low molecular weight organic acids in Arctic aerosol. *Sci. Total Environ.* 763 <https://doi.org/10.1016/j.scitotenv.2020.142954>.
- Ferrero, L., Cappelletti, D., Busetto, M., Mazzola, M., Lupi, A., Lanconelli, C., Becagli, S., Traversi, R., Caiazzo, L., Giardi, F., Moroni, B., Crocchianti, S., Fierz, M., Mocnik, G., Sangiorgi, G., Perrone, M., Maturilli, M., Vitale, V., Udisti, R., Bolzucchini, E., 2016. Vertical profiles of aerosol and black carbon in the Arctic: a seasonal phenomenology along 2 years (2011–2012) of field campaigns. *Atmos. Chem. Phys.* 16, 12601–12629. <https://doi.org/10.5194/acp-16-12601-2016>.
- Grannas, A.M., Bogdal, C., Hageman, K.J., Halsall, C., Harner, T., Hung, H., Kallenborn, R., Klán, P., Klánová, J., Macdonald, R.W., Meyer, T., Wania, F., 2013. The role of the global cryosphere in the fate of organic contaminants. *Atmos. Chem. Phys.* 13, 3271–3305. <https://doi.org/10.5194/acp-13-3271-2013>.
- Jaffrezzo, J.L., Clain, M.P., Masclat, P., 1994. Polycyclic aromatic hydrocarbons in the polar ice of Greenland. *Geochemical use of these atmospheric tracers. Atmos. Environ.* 28, 1139–1145. [https://doi.org/10.1016/1352-2310\(94\)90291-7](https://doi.org/10.1016/1352-2310(94)90291-7).
- Kallenborn, R., Brorström-Lundén, E., Reiersen, L.O., Wilson, S., 2017. Pharmaceuticals and personal care products (PPCPs) in Arctic environments: indicator contaminants for assessing local and remote anthropogenic sources in a pristine ecosystem in change. *Environ. Sci. Pollut. Res.* 1–13. <https://doi.org/10.1007/s11356-017-9726-6>.
- Katsoyiannis, A., Breivik, K., 2014. Model-based evaluation of the use of polycyclic aromatic hydrocarbons molecular diagnostic ratios as a source identification tool. *Environ. Pollut.* 184, 488–494. <https://doi.org/10.1016/j.envpol.2013.09.028>.
- Kawamura, K., Suzuki, I., 1994. Ice core record of Polycyclic Aromatic hydrocarbons over the Past 400 Years. *Naturwissenschaften* 81, 502–505.
- Kim, J.H., Peterse, F., Willmott, V., Klitgaard Kristensen, D., Baas, M., Schouten, S., Sinnighe Damsté, J.S., 2011. Large ancient organic matter contributions to Arctic marine sediments (Svalbard). *Limnol. Oceanogr.* 56, 1463–1474. <https://doi.org/10.4319/lo.2011.56.4.1463>.
- Kosek, K., Kozak, K., Kozioł, K., Jankowska, K., Chmiel, S., Polkowska, Ż., 2018. The interaction between bacterial abundance and selected pollutants concentration levels in an arctic catchment (southwest Spitsbergen, Svalbard). *Sci. Total Environ.* 622 (623), 913–923. <https://doi.org/10.1016/j.scitotenv.2017.11.342>.
- Kozak, K., Polkowska, Ż., Ruman, M., Kozioł, K., Namieśnik, J., 2013. Analytical studies on the environmental state of the Svalbard Archipelago provide a critical source of information about anthropogenic global impact. *TrAC, Trends Anal. Chem.* 50, 107–126. <https://doi.org/10.1016/j.trac.2013.04.016>.
- Kozak, K., Ruman, M., Kosek, K., Karasiński, G., Stachnik, Ł., Polkowska, Ż., 2017. Impact of Volcanic Eruptions on the Occurrence of PAHs Compounds in the Aquatic Ecosystem of the Southern Part of West Spitsbergen (Hornsund Fjord, Svalbard), vol. 9. <https://doi.org/10.3390/w9010042>. Water (Switzerland).
- Kozioł, K., Kozak, K., Polkowska, Ż., 2017. Hydrophobic and hydrophilic properties of pollutants as a factor influencing their redistribution during snowpack melt. *Sci. Total Environ.* 596 (597), 158–168. <https://doi.org/10.1016/j.scitotenv.2017.04.061>.
- Law, K.S., Stohl, A., 2007. *Arctic Air Pollution : Origins and Impacts.* sc 315, 1537–1541.
- Lebedev, A.T., Mazur, D.M., Polyakova, O.V., Kosyakov, D.S., Kozhevnikov, A.Y., Latkin, T.B., Andreeva Yu, I., Artaev, V.B., 2018. Semi volatile organic compounds in the snow of Russian Arctic islands: archipelago Novaya Zemlya. *Environ. Pollut.* 239, 416–427. <https://doi.org/10.1016/j.envpol.2018.03.009>.
- Lehmann-Konera, S., Ruman, M., Franczak, Ł., Polkowska, Ż., 2020. Contamination of Arctic Lakes with Persistent Toxic Pah Substances in the NW Part of Wedell Jarlsberg Land (Bellsund, Svalbard). *Water (Switzerland)*, vol. 12. <https://doi.org/10.3390/w12020411>.
- Lei, Y.D., Wania, F., 2004. Is rain or snow a more efficient scavenger of organic chemicals? *Atmos. Environ. Times* 38, 3557–3571. <https://doi.org/10.1016/j.atmosenv.2004.03.039>.
- Li, R., Gao, H., Ji, Z., Jin, S., Ge, L., Zong, H., Jiao, L., Zhang, Z., Na, G., 2020. Distribution and sources of polycyclic aromatic hydrocarbons in the water column of Kongsfjorden, Arctic. *J. Environ. Sci. (China)* 97, 186–193. <https://doi.org/10.1016/j.jes.2020.04.024>.
- Macdonald, R.W., Barrie, L.A., Bidleman, T.F., Diamond, M.L., Gregor, D.J., Semkin, R.G., Strachan, W.M., Li, Y.F., Wania, F., Alae, M., Alexeeva, L.B., Backus, S.M., Bailey, R., Bowers, J.M., Gobeil, C., Halsall, C., Harner, T., Hoff, J.T., Jantunen, L.M., Lockhart, W.L., Mackay, D., Muir, D.C.G., Pudykiewicz, J., Reimer, K.J., Smith, J.N., Stern, G. a., 2000. Contaminants in the Canadian Arctic: 5 years of progress in understanding sources, occurrence and pathways. *Sci. Total Environ.* 254, 93–234.
- Masclat, P., Hoyau, V., Jaffrezzo, J.L., Cachier, H., 2000. Polycyclic aromatic hydrocarbon deposition on the ice sheet of Greenland. Part I: Superficial snow. *Atmos. Environ.* 34, 3195–3207. [https://doi.org/10.1016/S1352-2310\(99\)00196-X](https://doi.org/10.1016/S1352-2310(99)00196-X).
- Melnikov, S., Carroll, J., Gorshkov, a, Vlasov, S., Dahle, S., 2003. Snow and ice concentrations of selected persistent pollutants in the Ob-Yenisey river watershed. *Sci. Total Environ.* 306, 27–37. [https://doi.org/10.1016/S0048-9697\(02\)00482-5](https://doi.org/10.1016/S0048-9697(02)00482-5).
- Meyer, T., Wania, F., 2008. Organic contaminant amplification during snowmelt. *Water Res.* 42, 1847–1865. <https://doi.org/10.1016/j.watres.2007.12.016>.
- Na, G., Liang, Y., Li, R., Gao, H., Jin, S., 2021. Flux of Polynuclear aromatic compounds (PAHs) from the atmosphere and from Reindeer/Bird feces to arctic soils in Ny-Ålesund (svalbard). *Arch. Environ. Contam. Toxicol.* 81, 166–181. <https://doi.org/10.1007/s00244-021-00851-1>.
- Oehme, M., Haugen, J.-E., Schlabach, M., 1996. Seasonal changes and relations between levels of organochlorines in arctic ambient air: first results of an all-year-round monitoring program at Ny-Alesund, Svalbard, Norway. *Environ. Sci. Technol.* 30, 2294–2304. <https://doi.org/10.1021/es950701+>.
- Polkowska, Ż., Cichala-Kamrowska, K., Ruman, M., Kozioł, K., Krawczyk, W.E., Namieśnik, J., 2011. Organic pollution in surface waters from the Fuglebekken basin in Svalbard, Norwegian Arctic. *Sensors* 11, 8910–8929. <https://doi.org/10.3390/s110908910>.
- Pouch, A., Zaborska, A., Pazdro, K., 2017. Concentrations and origin of polychlorinated biphenyls (PCBs) and polycyclic aromatic hydrocarbons (PAHs) in sediments of western Spitsbergen fjords (Kongsfjorden, Hornsund, and Adventfjorden). *Environ. Monit. Assess.* 189, 175. <https://doi.org/10.1007/s10661-017-5858-x>.
- Spolaor, A., Varin, C., Pedeli, X., Christille, J.M., Kirchengoert, T., Giardi, F., Cappelletti, D., Turetta, C., Cairns, W.R.L., Gambaro, A., Bernagozzi, A., Gallet, J.C., Björkman, M.P., Barbaro, E., 2021. Source, timing and dynamics of ionic species mobility in the Svalbard annual snowpack. *Sci. Total Environ.* 751, 141640 <https://doi.org/10.1016/j.scitotenv.2020.141640>.
- Steenhuisen, F., van den Heuvel-Greve, M., 2021. Exposure radius of a local coal mine in an Arctic coastal system; correlation between PAHs and mercury as a marker for a local mercury source. *Environ. Monit. Assess.* 193, 1–21. <https://doi.org/10.1007/s10661-021-09287-5>.
- Stein, A.F., Draxler, R., Rolph, G.D., Stunder, B.J.B., Cohen, M.D., Ngan, F., 2015. NOAA's HYSPLIT atmospheric transport and dispersion modeling system. *Bull. Am. Meteorol. Soc.* 96, 2059–2077.



- Stohl, A., Berg, T., Burkhart, J.F., Fjæraa, A.M., Forster, C., Herber, A., Hov, Ø., Lunder, C., McMillan, W.W., Oltmans, S., Shiobara, M., Simpson, D., Solberg, S., Stebel, K., Ström, J., Tørseth, K., Treffeisen, R., Virkkunen, K., Yttri, K.E., 2007. Arctic smoke – record high air pollution levels in the European Arctic due to agricultural fires in Eastern Europe in spring 2006. *Atmos. Chem. Phys.* 7, 511–534. <https://doi.org/10.5194/acpd-6-9655-2006>.
- Sun, J., Shen, Z., Zhang, T., Kong, S., Zhang, H., Zhang, Q., Niu, X., Huang, S., Xu, H., Ho, K.F., Cao, J., 2022. A comprehensive evaluation of PM<sub>2.5</sub>-bound PAHs and their derivative in winter from six megacities in China: Insight the source-dependent health risk and secondary reactions. *Environ. Int.* 165, 107344 <https://doi.org/10.1016/j.envint.2022.107344>.
- Tobiszewski, M., Namieśnik, J., 2012. PAH diagnostic ratios for the identification of pollution emission sources. *Environ. Pollut.* 162, 110–119. <https://doi.org/10.1016/j.envpol.2011.10.025>.
- Vecchiato, M., Barbaro, E., Spolaor, A., Burgay, F., Barbante, C., Piazza, R., Gambaro, A., 2018. Fragrances and PAHs in snow and seawater of Ny-Ålesund (Svalbard): local and long-range contamination. *Environ. Pollut.* 242, 1740–1747. <https://doi.org/10.1016/j.envpol.2018.07.095>.
- Vecchiato, M., Gambaro, A., Kehrwald, N.M., Ginot, P., Kutuzov, S., Mikhalenko, V., Barbante, C., 2020. The Great Acceleration of fragrances and PAHs archived in an ice core from Elbrus, Caucasus. *Sci. Rep.* 10, 1–10. <https://doi.org/10.1038/s41598-020-67642-x>.
- Vehviläinen, J., Isaksson, E., Moore, J.C., 2002. A 20th-century record of naphthalene in an ice core from Svalbard. *Ann. Glaciol.* 35, 257–260. <https://doi.org/10.3189/172756402781817329>.
- Xie, Z., Wang, Z., Mi, W., Möller, A., Wolschke, H., Ebinghaus, R., 2015. Neutral Poly-/perfluoroalkyl Substances in air and snow from the arctic. *Sci. Rep.* 5, 1–6. <https://doi.org/10.1038/srep08912>.
- Yu, Y., Katsoyiannis, A., Bohlin-Nizzetto, P., Brorström-Lundén, E., Ma, J., Zhao, Y., Wu, Z., Tych, W., Mindham, D., Sverko, E., Barresi, E., Dryfhout-Clark, H., Fellin, P., Hung, H., 2019. Polycyclic aromatic hydrocarbons not declining in arctic air despite global emission Reduction. *Environ. Sci. Technol.* 53, 2375–2382. <https://doi.org/10.1021/acs.est.8b05353>.
- Zhang, B., Sun, J., Jiang, N., Zeng, Y., Zhang, Y., He, K., Xu, H., Liu, S., Hang Ho, S.S., Qu, L., Cao, J., Shen, Z., 2021. Emission factors, characteristics, and gas-particle partitioning of polycyclic aromatic hydrocarbons in PM<sub>2.5</sub> emitted for the typical solid fuel combustions in rural Guanzhong Plain, China. *Environ. Pollut.* 286, 117573 <https://doi.org/10.1016/j.envpol.2021.117573>.
- Zhang, Y., Shen, Z., Sun, J., Zhang, L., Zhang, B., Zhang, T., Wang, J., Xu, H., Liu, P., Zhang, N.N., Cao, J., 2020. Parent, alkylated, oxygenated and nitro polycyclic aromatic hydrocarbons from raw coal chunks and clean coal combustion: emission factors, source profiles, and health risks. *Sci. Total Environ.* 721, 137696 <https://doi.org/10.1016/j.scitotenv.2020.137696>.